Science of the Total Environment 853 (2022) 158662

Contents lists available at ScienceDirect

Science of the Total Environment

journal homepage: www.elsevier.com/locate/scitotenv

Salinity reduces site quality and mangrove forest functions. From monitoring to understanding

Shamim Ahmed [a,b,*], Swapan Kumar Sarker [c], Daniel A. Friess [d], Md. Kamruzzaman [b], Martin Jacobs [a], Md. Akramul Islam [e], Md. Azharul Alam [f], Mohammad Jamil Suvo [g], Md. Nasir Hossain Sani [h], Tanmoy Dey [e], Clement Sullibie Saagulo Naabeh [i], Hans Pretzsch [a]

[a] Chair of Forest Growth and Yield Science, Department of Life Science Systems, School of Life Sciences, Technical University of Munich, Hans-Carl-von-Carlowitz-Platz 2, 85354 Freising, Germany
[b] Forestry and Wood Technology Discipline, Khulna University, Khulna 9208, Bangladesh
[c] Department of Forestry and Environmental Science, Shahjalal University of Science and Technology, Sylhet, Bangladesh
[d] Department of Geography, 1 Arts Link, National University of Singapore, 117570, Singapore
[e] Bangladesh Forest Research Institute, Ministry of Environment, Forest and Climate Change, Bangladesh
[f] Department of Pest Management and Conservation, Lincoln University, Lincoln 7647, New Zealand
[g] Faculty of Agricultural Sciences, Nutritional Science and Environmental Management, Justus Liebig University, Bismarckstraße 24, 35390 Giessen, Germany
[h] School of Natural Sciences, Bangor University, Gwynedd LL57 2UW, UK
[i] Institute of Environment and Sanitation Studies, University of Ghana, International Programmes Office, MR39 + C4X, Annie Jiagge Rd, Accra, Ghana

HIGHLIGHTS

- Ecosystem responses to salinity gradients were studied in the Bangladesh Sundarbans.
- Increasing salinity significantly impedes forest growth and ecosystem functions.
- Nutrients and leaf area index had a positive impact on functional variables.
- The power law explains the consistent decline of functional variables with salinity.
- High nutrient availability and leaf area are likely to buffer the salinity impacts.

GRAPHICAL ABSTRACT

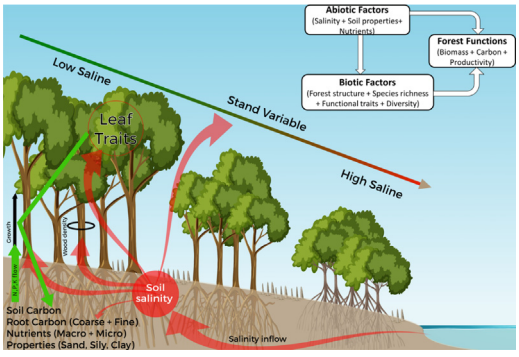

ARTICLE INFO

Editor: Elena Paoletti

Keywords:
Carbon pools
Nutrients
Functional traits
Growth dominance
Growth reduction
Dwarfism

ABSTRACT

Mangroves continue to be threatened across their range by a mix of anthropogenic and climate change-related stress. Climate change-induced salinity is likely to alter the structure and functions of highly productive mangrove systems. However, we still lack a comprehensive understanding of how rising salinity affects forest structure and functions because of the limited availability of mangrove field data. Therefore, based on extensive spatiotemporal mangrove data covering a large-scale salinity gradient, collected from the world's largest single tract mangrove ecosystem – the Bangladesh Sundarbans, we, aimed to examine (QI) how rising salinity influences forest structure (e.g., stand density, diversity, leaf area index (LAI), etc.), functions (e.g., carbon stocks, forest growth), nutrients availability, and functional traits (e.g., specific leaf area, wood density). We also wanted to know (QII) how forest functions interact (direct vs. indirect) with biotic (i.e., stand structure, species richness, etc.) and abiotic factors (salinity, nutrients, light availability, etc.). We also asked (QIII) whether the functional variable decreases disproportionately with salinity and applied the power-law (i.e., $Y = a X^b$) to the salinity and functional variable relationships. In this study, we found that

* Corresponding author at: Chair of Forest Growth and Yield Science, Department of Life Science Systems, School of Life Sciences, Technical University of Munich, Hans-Carl-von-Carlowitz-Platz 2, 85354 Freising, Germany.
E-mail address: shamim.ahmed@tum.de (S. Ahmed).

http://dx.doi.org/10.1016/j.scitotenv.2022.158662
Received 26 July 2022; Received in revised form 6 September 2022; Accepted 6 September 2022
Available online 8 September 2022

rises in salinity significantly impede forest growth and produce less productive ecosystems dominated by dwarf species while reducing stand structural properties (i.e., tree height, basal area, dominant tree height, LAI), soil carbon (organic and root carbon), and macronutrient availability in the soil (e.g., NH4 +, P, and K). Besides, species-specific leaf area (related to resource acquisition) also decreased with salinity, whereas wood density (related to resource conservation) increased. We observed a declining abundance of the salt-intolerant climax species (*Heritiera fomes*) and dominance of the salt-tolerant species (*Excoecaria agallocha*, *Ceriops decandra*) in the high saline areas. In the case of biotic and abiotic factors, salinity and salinity-driven gap fraction (high transmission of light) had a strong negative impact on functional variables, while nutrients and LAI had a positive impact. In addition, the power-law explained the consistent decline of functional variables with salinity. Our study disentangles the negative effects of salinity on site quality in the Sundarbans mangrove ecosystem, and we recognize that nutrient availability and LAI are likely to buffer the less salt-tolerant species to maintain the ability to sequester carbon with sea-level rise. These novel findings advance our understanding of how a single stressor—salinity—can shape mangrove structure, functions, and productivity and offer decision makers a much-needed scientific basis for developing pragmatic ecosystem management and conservation plans in highly stressed coastal ecosystems across the globe.

1. Introduction

Mangrove forests are among the most dynamic and distinctive coastal ecosystems, ranging mostly in the tropics and subtropics (covering 0.7 % and 0.1 % of tropical and world forests, respectively) (Friess et al., 2019; Giri et al., 2011; Thomas et al., 2017). They are among the most carbon-rich forests on earth, storing up to five times more carbon per unit area than any other forested ecosystem (Donato et al., 2011; Friess, 2019). Mangroves provide an array of ecosystem services, including protection from extreme weather events, regulating global climate, as well as livelihoods and aesthetic values for millions of coastal people by providing food, building materials, and ecotourism (reviewed in Friess et al. (2020)).

However, mangrove forests have been severely degraded, defaunated, and fragmented globally in recent decades due to anthropogenic threats such as deforestation for land conversion and timber, resource over-exploitation, and pollution (Friess et al., 2019). Importantly, climate change-induced biophysical pressures on mangroves, such as cyclones, erosion, sea-level rise, salinization, etc., have increased since the early 21st century (Carugati et al., 2018; Goldberg et al., 2020; Hamilton and Casey, 2016; Lee et al., 2021; Richards and Friess, 2016). Specifically, increasing salinity due to sea-level rise makes mangrove forests more vulnerable in many tropical regions (Kirwan and Megonigal, 2013). Due to remaining at the interface of land and sea, salinity is recognized as one of the key ecosystem controlling factors in mangroves (Chen and Wang, 2017). Similarly, the Sundarbans mangrove forest (SMF) is located at the interface of land and sea in an active delta (i.e., Ganges-Brahmaputra) and largely exposed to the sea where sedimentation is still occurring (Mukhopadhyay et al., 2018), which makes SMF more vulnerable to increasing salinity. For example, Sarker et al. (2019a) predicted that the SMF is becoming more homogeneous by losing species under constant habitat deterioration. Alarmingly, Sarker et al. (2021) predicted a 50 % salinity increase by 2050 could reduce overall ecosystem productivity by 30 %. Such large increases in salinity are possible, as there has been a 90 % reduction in freshwater discharge into the SMF since 1975 due to upstream dam construction (Aziz and Paul, 2015), encouraging salt-tolerant species to survive (Banerjee et al., 2017). Although few studies have shown that mangrove species typically display inherent eco-physiological resilience against deteriorated environments through acclimatisation (Begam et al., 2020; Ellison, 2015). But, the information how overall mangrove ecosystem will react to salinity and climate change is scarce.

There is a strong body of evidence that rapid changes in salinity can negatively impact mangrove forest distribution, productivity, and growth (Peters et al., 2020; Yoshikai et al., 2021). The impact may vary depending on meteorological variables, light intensity, species-specific physiological responses, and soil conditions. For example, higher salinity may force the forest to homeostasis collapse by restricting normal functional processes of the forest (Chowdhury et al., 2019) by limiting the release of nutrients by inhibiting microbial decomposers, which may further alter species distribution and composition (Alongi, 2018). A recent study conducted in the SMF showed that soil salinity, pH, and siltation are the major mangrove biodiversity-restricting factors (Sarker et al., 2019b), but the underlying mechanisms of how they reduce forest functions are poorly understood. In addition to salinity, several biotic and abiotic factors can influence forest functions. To illustrate, nutrient availability largely controlled mangrove growth and the biotic and abiotic factor interactions (e.g., direct vs indirect) (Reef et al., 2010) and species diversity enhances carbon stocks (Rahman et al., 2021a). Indeed, species richness is closely related to the productivity and nutrient cycling of an ecosystem (Ratcliffe et al., 2017; Tilman et al., 1997). In addition, structural diversity such as variation in height enhances our ability to better predict ecosystem functions under stress (LaRue et al., 2019; Tilman et al., 1997) and is further linked to diversity productivity relationships through niche complementarity and light-capturing (Zheng et al., 2019). Hence, uncovering the relationships between these factors may enhance our understanding of how the ecosystem functions (Huang et al., 2018) to stress. These complex interactions between the biotic and abiotic factors with forest functions and their relative importance in mangroves incorporating salinity are not well documented or rarely focused.

Several studies across the globe have already attempted to assess the impact of salinity, mostly on blue carbon and stand structure of mangroves (Alongi, 2022; Rahman et al., 2021a; Sarker et al., 2019b), but rarely uncovered overall ecosystem reactions to climate change. A few studies have examined salinity eco-zone impacts on forest structure (Ahmed and Kamruzzaman, 2021; Kamruzzaman et al., 2017), above-ground carbon stocks (Rahman et al., 2015), soil carbon (Rahman et al., 2021b), fine root (Ahmed et al., 2021) in the SMF. However, we lack a comprehensive quantitative understanding of how rising salinity may affect overall mangrove structure and functions. This knowledge gap comes from the limited fine-scale salinity data availability (rarely focused on a large-scale salinity gradient) and its effect on species down to the community-level (e.g., mangrove structure, functions, growth and productivity). The knowledge gap limits our ability to better predict mangroves' structural and functional dynamics under changing climates. Apart from this, the increasing salinity trend may support our expected interactions with other forest factors, to illustrate, salinity negatively affects forest variables, and diversity positively affects functions. To date, how salinity mediates the relationships between productivity and other forest variables in mangrove forests is still an open question specifically across a large-scale salinity gradient.

Moreover, it is well recognized that blue carbon is impacted by salinity (Rahman et al., 2015; Rahman et al., 2021a), which raises new questions about whether salinity-modified functional variables follow the power-law (i.e., $Y = a X^b$ or $\log Y = \log a + b \log X$) or not, which is critical to explain how one variable potentially impacts other variables (Duncanson et al., 2015). Exploring these consistent patterns provides crucial key information for understating forest dynamics (Farrior et al., 2016) and can be linked with metabolic scaling theory (MST) predictions (i.e., various size and shape should scale one another) (Jucker et al., 2022; Shenkin et al., 2020). There are several examples in forest ecology that follow power-law distribution such as tree height and diameter relationships ($H \propto D^{2/3}$)

(Duncanson et al., 2015; Jucker et al., 2022), and tree-size distribution (i.e., dominant and suppressed) (Farrior et al., 2016), but not commonly seen to use in functional variables and in mangrove. We thus assume that a consistent decline in functional variables (e.g., forest growth and carbon pools) with rising salinity can be scaled by a power law as forest functions largely defined by structure and thus related to MST. We aimed to simplify the salinity and functional variables relationships in mangroves which may help to better understand mangrove eco-physiological response, carbon dynamics and MST predictions. Therefore, considering the determining role of salinity together with other forest variables, we comprehensively investigated the interactive effects of increasing soil salinity (a large-scale salinity) on mangrove productivity and associated ecosystem functioning (growth and carbon pools), by taking species differences in salinity tolerance to accurately predict the mangrove biomass dynamics.

However, limited location specific data restricts our understanding of mangrove dynamics (Dasgupta et al., 2019). Based on exhaustive spatio-temporal mangrove data collected from the SMF, the overarching aim of this study was to understand how rising salinity influences multiple fundamental aspects of a mangrove forest (i.e., structure, functions, growth, and productivity). Therefore, we ask (QI) what are the responses of the forest variables, functional traits, and growth patterns to the salinity gradient and between the salinity ecozones (low vs. high magnitude of salinity)? (QII) what are the relationships between abiotic (salinity, nutrients, etc.), biotic factors (stand structure, species richness, etc.), and functional variables (forest growth and carbon stocks) along the salinity gradient? and (QIII) does the power law apply to salinity-modified ecosystem functional variables such as growth and carbon pools?

Precisely, we posed the following three hypotheses: (HI) salinity impacts the forest variables negatively which is shown in Fig. 1 and shifts the growth trend from positive to negative. (HII) Salinity would have direct negative impacts on forest variables while species and structural diversity and nutrients might have positive impacts and these relationships may have varied across the salinity gradient and zones. (HIII) We hypothesized that forest functional variables would decline consistently and proportionately with increasing salinity, implying that the power-law would be supported.

To answer the questions and test the hypotheses, we evaluated forest structure, species, and structural diversity, carbon pools (above and belowground), nutrient contents, and functional traits (specific leaf area and wood density).

2. Materials and methods

2.1. Study site description

Located in the Gangetic delta between Bangladesh (60 % of the mangrove forest area or 6017 km^2) and India (40 %), and comprising nearly half of the world's mangrove plant species, the Sundarbans serves as a bio-shield and provides the livelihood for around 3.5 million people (Abdullah et al., 2016; Hamilton and Casey, 2016; Rahman and Begum, 2011; Uddin et al., 2013). However, this global priority mangrove ecosystem is severely imperilled by climate change and anthropogenic disturbances (Halder et al., 2021; Hamilton and Casey, 2016; Rahman, 2020). Notably, Bangladesh's coastline is experiencing a higher rate of sea-level rise (5.93 mm yr^{-1}) than the rest of the world (1.0–2.0 mm yr^{-1}) (Karim and Mimura, 2008), as 50 % of the land remains 8 m below sea level (Mörner, 2010). Thus, the Bangladesh Sundarbans mangrove forest (SMF) is more susceptible to salinity intrusion (Sarker et al., 2016) with alterations in hydrological patterns (Wahid et al., 2007) and soil biogeochemistry (Banerjee et al., 2017).

We conducted this study in the Sundarbans mangrove forest (SMF), Bangladesh (21°30′–22° 30′ N, 89°00′–89°55′ E) (Supplementary Fig. 1, and Islam (2001)). A river water salinity characterization classifies the ecosystem into three major unique ecological zones, namely, oligohaline, mesohaline, and polyhaline with salinities of <14 ppt, 14–25 ppt, and >25 ppt respectively (Islam and Gnauck, 2009). These salinity ecozones strongly influence the plant communities in SMF (Ahmed and Iqbal, 2011).

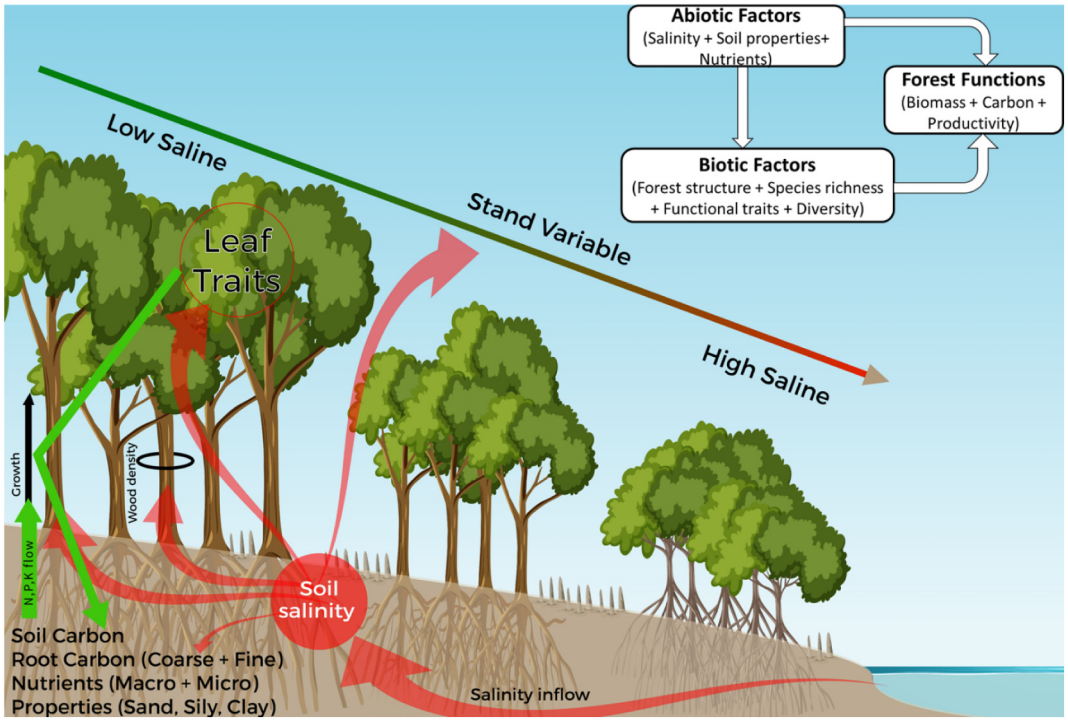

Fig. 1. Visualization of the link between salinity and forest variables (above and belowground). An inset depicting the relationship between biotic, abiotic, and forest functions is provided. The negative effects are indicated by the red arrow. Growth is defined by a black, solid vertical line and the circle denotes wood density at 1.3 m. Red lines indicate negative and green lines indicate positive impacts.

2.2. Tree inventory

To evaluate forest variables and carbon stocks, we established 60 permanent sample plots (PSPs). Each plot measured 0.01 ha and 20 PSPs were established in each of the salinity eco-regions by adopting a stratified random sampling technique across the SMF in April 2018. The plots represented the forest types (Iftekhar and Saenger, 2008) in the oligohaline (*Heritiera fomes, H. fomes – Excoecaria agallocha*, and *E. agallocha – H. fomes*), mesohaline (*H. fomes – E. agallocha*, and *E. agallocha – H. fomes*) and polyhaline (*E. agallocha – Ceriops decandra* and the *C. decandra – E. agallocha*) eco-regions (Supplementary Fig. 1). We identified and tagged all the trees with DBH (diameter at breast height – 1.3 m from the ground) ≥ 4.6 cm with an aluminium tag and also measured tree heights using an electrical Dendrometer (Criterion RD 1000, Laser Technology Incorporation, USA). Because of the sluggish growth pattern of mangroves especially aboveground, we adopted the criterion (4.6 cm) that has been used since the 1900s (Iftekhar and Saenger, 2008). Trees with DBH ≤ 4.6 cm were marked as seedlings or regeneration and counted by species name by establishing a 2 m × 5 m plot at the center of each PSP (Supplementary Fig. 2). We revisited all the PSPs in November 2020 and measured DBH and heights of all trees (in total 1378) tagged in 2018 to evaluate growth (biomass changes over time) and changes in growth dominance pattern with salinity. We acquired five elevation readings (above mean sea level) from each PSP using the established digital elevation model developed by (IWM, 2003) for the SMF (vertical accuracy at pixel level: ±1 m) and then averaged these readings to minimize the error associated with the digital elevation model.

2.3. Stand structure, species, and structural diversity

We used all measured (DBH ≥ 4.6 cm) trees to calculate stand characteristics such as stand density (stems ha^{-1}); mean tree height (m), quadratic mean diameter at breast height (DBH) (or at 130 cm), stand basal area (m^2/ha), and the mean height of top tall 20 % trees of the plot i.e., dominant height (m). To characterize species diversity, we used Shannon's index because this index gives similar weights on both species' frequency and dominancy, thus not favoring any species disproportionately (Hortal et al., 2010; Jost, 2006; Liu et al., 2018). In terms of structural diversity (size class distributions) (vertical and horizontal), we again used Shannon's index by replacing species with height classes (1 m interval) and DBH classes (2 cm interval), respectively. We measured LAI and canopy gap fraction (the amount of the sky visible from beneath the canopy and indicates the fraction of canopy foliage cover) using the CI-100 plant canopy analyzer (CID Bio-Science, USA). To account for plot-level variability, we obtained five LAI and gap fraction/Transmission Coefficient readings from each PSP and averaged the readings.

2.4. Above ground biomass and carbon estimation

We used a non-destructive method (e.g., allometry equations) to estimate tree aboveground biomass. We obtained local allometric equations for dry biomass estimation of all tree species that were recently proposed by Rahman et al. (2021c) (see Supplementary Table 1) and later converted into aboveground carbon (i.e., multiplying by 0.5) following Gifford (2000).

2.5. Soil carbon and nutrients

We employed a soil sample design to account for within-plot spatial variability in soil properties, below-ground nutrients, and carbon (soil and root) (Supplementary Fig. 2a) and collected a total of nine soil samples from each PSP at varying depths (15 cm for nutrients and properties; 50 cm for root and soil organic carbon (SOC)) (Supplementary Fig. 2a). We collected one sample from the center of each PSP to analyze soil texture (Supplementary Fig. 2a). We used the hydrometer method to determine the soil texture (% of sand, silt, and clay) (Gee and Bauder, 1986) and observed almost identical patterns up to 15 cm of soil depth (Supplementary Fig. 3). We used a soil conductivity meter (Extech 341350A-P Oyster) to determine in situ soil salinity (as electrical conductivity-EC) in a 1: 5 distilled water: soil dilution (adopted from Sarker (2017)) once the tidal water level stabilized to avoid tidal effect on salinity. Later, we measured in-field soil pH using a digital soil pH meter.

Denitrification transforms nitrate into ammonia, making ammonium the most abundant nitrogen source in mangroves (reviewed in Reef et al. (2010)). Therefore, we selected and measured soil NH_4^+ concentration following the Kjeldahl method (Bremner and Breitenbeck, 1983). The molybdovanadate method was used to quantify total phosphorus (P) using a spectrophotometer. Sulphide (S) concentrations were measured using an UV–Vis Spectrophotometer. We used a hollow cathode lamp (HCL) and the automatic mode in an atomic absorption spectrophotometer (AA-7000) to quantify potassium (K) concentrations. Besides, magnesium (Mg), iron (Fe), zinc (Zn), and copper (Cu) concentrations in soil were measured using the atomic absorption spectrophotometer at the soil chemistry laboratory of the Civil and Environmental Engineering Department at the Shahjalal University of Science and Technology, Bangladesh. Overall nutrients analyses were adopted from Sarker (2017). We collected a total of 120 samples for soil and root carbon (two from each plot), one sample from the center of each plot for soil properties analysis while 240 samples collected (four from each plot) were samples for nutrient analysis.

2.5.1. Soil organic carbon

Mangroves are among the most dynamic carbon-rich coastal ecosystems, storing up to five times more soil carbon per unit area than any other forested ecosystem (Donato et al., 2011; Friess, 2019). The river-dominated Sundarbans ecosystem receives organic matter from both allochthonous (e.g., riverine loadings) and autochthonous sources (e.g., mangrove litter, above-ground roots, benthic vegetation, etc.) (Ray et al., 2018). Most of the areas in the Sundarbans is washed by the tide twice a day. While such tides transport sediments and high allochthonous input in the regularly inundated areas (i.e., near-sea southern and western Sundarbans), the relatively elevated areas (i.e., species-rich northern and north-eastern Sundarbans) which are only inundated by spring tides foster autochthonous SOC (Rahman et al., 2021b).

We estimated Soil Organic Carbon (SOC) following the methods described by Howard et al. (2014). We collected two soil samples per plot (total 120) by an auger (open-faced, diameter 5.6 cm and length 1.2 m), and divided them into four soil depths classes (0–10, 10–20, and 20–50 cm) following. Soil subsamples (2 cm) were taken from the middle of each class, transferred into plastic zipper bags after removing all stones, visible roots, branches, and twigs, and finally stored in a temperature-controlled (lower 10 °C) thick plastic box to avoid further oxidation and microbial decomposition, before sending them to the laboratory for the analysis. In the laboratory, around 50 mg of soil was passed through the elemental analyzer (Thermo 215 Scientific Flash 2000-NC Soil Analyzer) and inorganic carbon was separated to derive SOC following the protocols recommended for standard titration methods (Rahman et al., 2021b).

2.5.2. Soil root (coarse and fine) carbon

We sampled the living tree roots from the top 50 cm of soil depth using the soil-core method to estimate belowground root carbon. The soil-core method is recommended for its cost-effectiveness, accuracy, and less time and labor requirements (Addo-Danso et al., 2016). The depth of 30 cm is considered the most active soil layer for most mangrove root processes (Castañeda-Moya et al., 2011; Komiyama et al., 1987). A stainless-steel corer (internal diameter 12 cm and length 57 cm) was used to gather two soil cores (total 120) within each sample plot (Supplementary Fig. 2a). It was promptly rinsed with 0.3 mm steel mesh and with river water then stored in polythene zipper bags for lab analysis. In the laboratory, the washed roots were soaked in fresh water while flowing through different steel sieve meshes at the same time to separate the root into size classes, such as >2 mm (fine root) and >20 mm (coarse root). We followed the protocol of (Ahmed et al., 2021), using bare hands to distinguish living roots from deposited dead roots, as well as their

appearances. We weighed roots before and after oven-dried at 65^{0}C for 48 h, and all root biomass values were converted into carbon following Gifford (2000) and expressed as Mg C ha^{-1}.

2.6. Functional traits

Plant functional traits are crucial in terms of observing environmental changes (Damptey et al., 2022). Thus, along with other forest variables, we measured a few key functional traits: plant height, specific leaf area (SLA – leaf area per unit leaf mass), and wood density (WD – dry mass per unit volume of wood) (Conti and Díaz, 2013). Height, a whole-plant trait, is central to the carbon sequestration capacity of trees (Moles et al., 2009). SLA, a key trait of the "leaf economic spectrum" (Wright et al., 2005) regulates relative tree growth (Nicotra et al., 2010). WD is an important trait of the "wood economic spectrum" (Chave et al., 2009) that regulates tree hydraulics, architecture, defense, and growth potential (Poorter et al., 2010). Denser wood offers mechanical support to tree stems, thus increasing trees' capacity to survive under acute salinity stress (Lasky et al., 2014; Lawson et al., 2015). All functional variables were measured following the standard protocols developed by (Perez-Harguindeguy et al., 2013). A total of nine tree species from different zones were selected for trait measurement (see the full list and species-specific number of samples in Supplementary Table 2). Sample size varied due to the availability of mature tree species within plots as we only cored mature trees (DBH > 8 cm). For each tree, we collected a wood sample and at least three mature leaves from sun-exposed branches for laboratory measurements. For SLA, (a) all the leaves were immediately weighed in the field after collection to obtain the fresh weight and then stored in a uniquely remarked polythene zipper bag, (b) photographed the leaves (by a digital Camera-Nikon D5500) to measure fresh leaf area (cm^2) (Adobe Photoshop CS6), (c) oven-dried the leaves for 72 h at 70 °C and measured dry mass (g) with a digital balance (precision level 0.001 g), and (d) calculated SLA as fresh leaf area (cm^2)/dry mass (g). For WD, we collected wood cores using an increment borer and calculated fresh wood core volume (cm^3) ($V = r^2l$, where r = core radius, and l = core length), oven-dried the wood cores for 72 h at 103 °C, followed by dry mass (g) measurement, and finally, estimated WD as dry mass/fresh wood volume.

2.7. Salinity and meteorological data

We measured plot-level soil salinity in five random samples in each plot (60 plots) during April (early rainy season), and November (early winter or dry season) each year throughout the study period (2018–2020) to avoid seasonal effects on salinity. In addition, we collected salinity data for the last 10 years (2011 − 2021) from the Bangladesh Forest Department (BFD). The BFD collected salinity data from their established 30 PSPs across different salinity eco-regions during April and November each year as a part of the national forest inventory (which were within the 500 m range from our PSPs). We took the advantage of it to check how salinity changed over the last decade. Additionally, we acquired meteorological data (rainfall, temperature, and air relative humidity) for the last 10 years from the Bangladesh Meteorological Department, Khulna branch, which is the nearest meteorological station to the SMF. Meteorological variables were measured every hour and averaged for days and months. Here we have only presented monthly mean climatic data (Supplementary Fig. 4). Overall rainfall and humidity remained constant while temperature showed a slightly increasing trend over recent decades (Supplementary Fig. 4 a-c) but salinity increased sharply (Supplementary Fig. 4d). This increase of salinity could happen due to the combined effect of sea-level rise and lower upstream water flow, and in the near future, salinization will be intensified (The_World_Bank, 2022).

2.8. Statistical analysis

Statistics for testing HI: to test the first hypothesis i.e., the salinity gradient and eco-regional (high vs. low magnitude of salinity) impacts on forest variables, we compared the variation of all the parameters among the salinity eco-regions performing one-way ANOVA (analysis of variances) followed by a post-hoc Tukey HSD test. The normality of the parameters was assessed by the Shapiro–Wilk test. Log transformed data was used when the data was not normally distributed (Zhang and Chen, 2015). In addition, we conducted bivariate regression analyses to assess the individual forest variable(s) response to salinity. Through bivariate relationships, we also checked the growth response to forest biotic and abiotic variables.

Statistics for testing HII: to understand the complex direct and indirect relationships and their interactions between salinity-modified forest variables, we developed a structural equation model (SEM) using the 'Lavaan' package in R (Rosseel, 2012). SEM was chosen for its ability to depict direct and indirect relationships (Grace et al., 2012).

Statistics for testing HIII: finally, to test the third hypothesis which is to check whether the functional variables decrease disproportionately and consistently with the salinity, we applied and fitted the power-law (i.e., $Y = a X^b$ or $\log Y = \log a + b \log X$) by using the 'poweRlaw' package in R (Gillespie, 2014).

All statistical analysis and visualizations were performed in the R environment (version 4.1.1) (www.cran.r-project.org).

3. Results

3.1. Salinity impacts on forest variables

All stand structural variables except stand density showed significant variation across salinity eco-regions (Fig. 2A). Mean tree height, mean DBH, tree basal area, and species vertical and horizontal diversity showed a decreasing pattern along the salinity eco-regions with the lowest values at the polyhaline or strong saline eco-region (Fig. 2A, a1-a6). In contrast, the Shannon species diversity index showed a significantly ($p < 0.05$) higher value under polyhaline conditions (Fig. 2A, a7). Moreover, all carbon stock-related variables significantly varied across the salinity eco-regions and decreased with higher salinity (Fig. 2B). The highest stock of soil organic carbon and root carbon was found in the oligohaline or less saline eco-region (Fig. 2B, b3-b7). Also, major soil nutrients such as NH_4^+, P, Zn, and S decreased significantly in higher saline areas (Fig. 2C, c1-c2, c5-c6), whereas magnesium (Mg) increased (Fig. 3C, c4), and K, and Fe showed no significant responses (Fig. 2C, c3, c7) to salinity changes. High salinity (i.e., polyhaline zone) significantly lowered the LAI (leaf area index) (Fig. 2D, d1) while the canopy gap fraction showed an increasing pattern with increased salinity (Fig. 2D, d2). The highest number of small trees was observed in the oligohaline or mesohaline eco-regions, and the reserved J-shaped curve implied a higher number of large trees in these eco-regions than in the polyhaline eco-region (Supplementary Fig. 5). All salinity ecoregion-wise values are represented as mean with standard deviation in Supplementary Table 3 and plot-wise summaries are presented in Supplementary Fig. 6.

Bivariate analyses revealed that forest growth and belowground carbon (i.e., soil organic carbon and root carbon), tree height, DBH, and dominant height of the top 20 % of trees, LAI, and nutrients (NH_4^+, P, and K) significantly decreased with higher salinity (Fig. 3, a-f, h, j-l). Separately, species richness and canopy gap fraction significantly increased with salinity (Fig. 3, g, i; $p > 0.05$). Forest structural diversity (horizontal and vertical), and stand density had no significant association with plot-level soil salinity (Supplementary Fig. 7, a-c).

We observed functional traits (i.e., specific leaf area and wood density) varied between salinity eco-regions at species levels with few exceptions (i.e., remained almost unchanged) (Fig. 4a, b). Overall, the wood density of all the tree species increased, while specific leaf areas (SLA) showed a decreasing trend with increasing salinity (Fig. 4b). The compositional percentage of the early successional (*S. apetala*) and late-successional climax species (*H. fomes*) substantially declined whereas the contribution of the disturbance specialists (i.e., *E. agallocha, C. decandra*) considerably increased in the polyhaline eco-region (Fig. 4c). In terms of

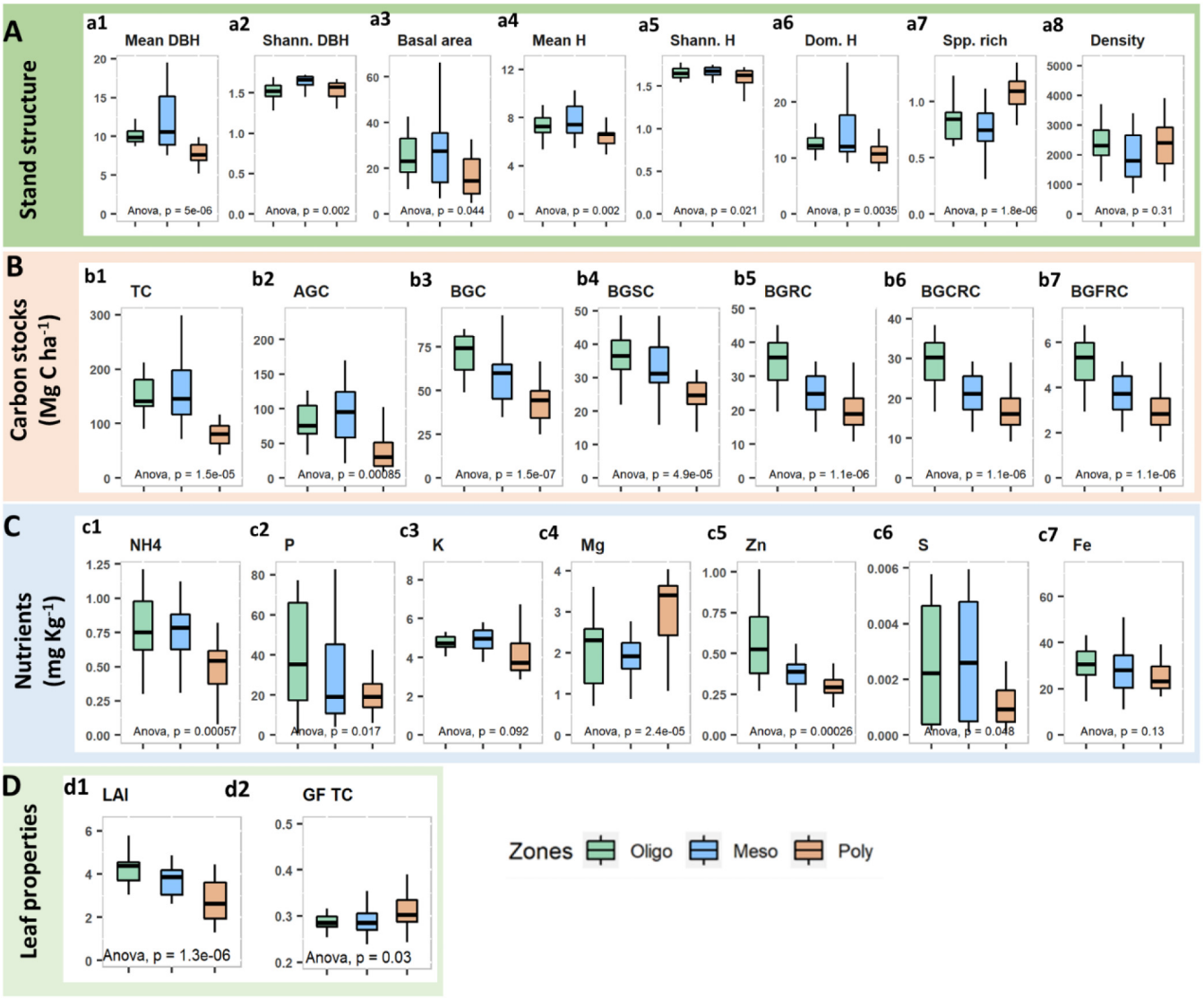

Fig. 2. The variation of forest variables across the three salinity eco-regions in the Sundarbans mangrove forest: oligohaline, mesohaline and polyhaline. (A) the stand's structural properties: (a1) average DBH (cm), (a2) horizontal diversity or Shannon DBH class richness, (a3) basal area (m2/ha), (a4) mean tree height (m), (a5) dominant height of the top 20 % of trees (m), (a6) vertical or Shannon height class diversity, (a7) species richness or Shannon species richness, (a8) stand density (tree/ha). (B) Carbon stocks: (b1) total carbon; TC, (b2) above ground carbon; AGC, (b3) total belowground carbon; BGC, (b4) belowground soil organic carbon; BGSC, (b5) belowground total root carbon; BGRC (20 mm) (BGCRC + BGGRC), (b6) belowground coarse root carbon; BGCRC (220 mm), (d) belowground fine root carbon; BGFRC (2 mm). (C) Nutrient contents: (c1) ammonium (NH4), (c2) phosphorus (P), (c3) potassium (K), (c4) magnesium (Mg), (c5) zinc (Zn), (c6) sulfur (S), (c7) iron (Fe). (D) leaf properties: (d1) leaf area index (LAI), (d2) gap fraction transmission coefficient (GFTC). Oligo, *meso*, and poly indicate low, medium, and high saline zones, respectively. The results of one-way ANOVA and the level of significance ($p < 0.05$) are shown in the inset.

natural regeneration success, *E. agallocha* outperformed all other species by contributing the highest counts of seedlings in all eco-regions (Fig. 4 d-e).

Biomass production over the ~2.5-year measurement period was significantly lower at higher salinities (Fig. 5a). In addition, the cumulative growth curve of living biomass changes throughout the measurement period (Fig. 5b) shows that when salinity rises, the biomass growth curve flattens, depicting the significant impact of rising salinity in slowing the growth in the polyhaline zone. Negative growth dominance patterns were identified across higher saline regions (Fig. 5c, d). Trees in oligohaline regions, on the other hand, mostly displayed positive growth dominance (Fig. 5c, d). Growth dominance patterns reveal that large tree growth was restricted but small-sized tree growth continued in higher saline ecozones and gradients (Fig. 5c and d).

Moreover, forest growth increased with tree height, DBH, stand density, leaf area index, and nutrient availability (i.e., N; P, K) (Supplementary Fig. 8 a-d, f-h). In contrast, increasing the canopy gap had a negative influence on forest growth (Supplementary Fig. 8e). However, horizontal and vertical structural diversity, and species diversity had no significant influence on forest growth across the different salinity eco-regions (Supplementary Fig. 7a-c).

3.2. Interactions between forest functions and abiotic and biotic factors

SEMs show the interactive relationships between soil salinity, growth, and other forest variables (Fig. 6, Supplementary Fig. 9). Overall, data showed that soil salinity had a negative effect on overall carbon pools, LAI, and nutrients (Fig. 6). Forest variables such as mean DBH, height, stand density, and salinity showed indirect associations (Fig. 6, Supplementary Fig. 9a). However, no direct significant associations were observed between soil salinity and growth, while salinity indirectly affected growth through the lens of leaf area index, carbon, nutrients, and canopy gap fraction (Fig. 6). Associations between soil salinity and other stand variables such as height, DBH, density, LAI, etc. largely varied among salinity zones (Supplementary Fig. 9c-d).

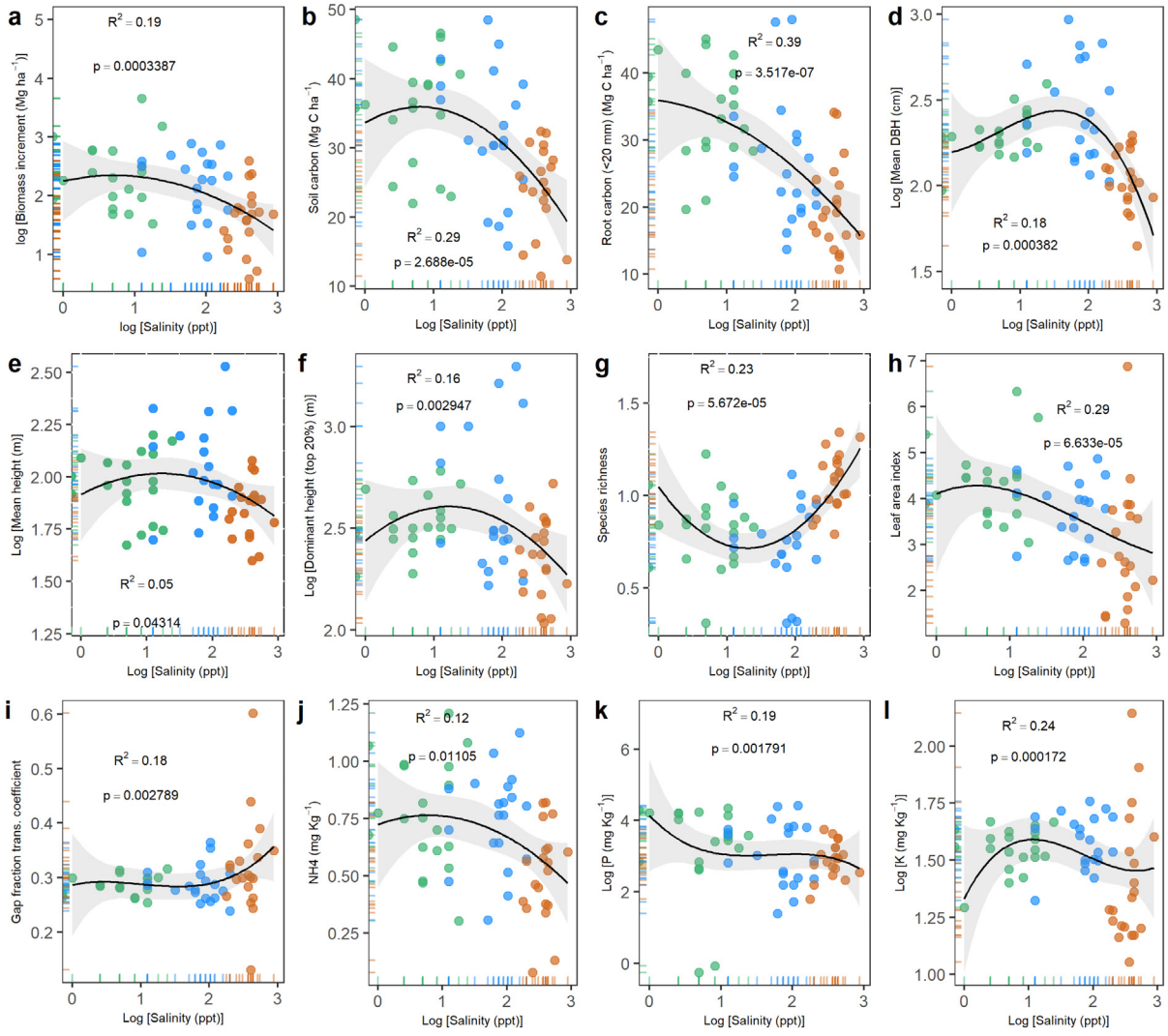

Fig. 3. Bivariate relationships between soil salinity and forest variables. (a) biomass increment, (b) soil carbon, (c) root carbon, (d) mean DBH, (e) mean height, (f) dominant height of top 20 % of tress, (g) species richness, (h) leaf area index, (i) canopy gap fraction, (j) NH_4^+, (k) Phosphorus (p), and (l) Potassium (k). Each colored point represents a sampling plot, while the black solid line indicates the fitted regression line (with R^2 value). The shaded area denotes the 95 % confidence interval. The rug plot along the axis margin displayed the distribution of the data with zero width bins. The *p*-value indicates the significance level at the 0.05 level. Colored points define the data from different salinity eco-regions: green, blue, and orange denote data from oligohaline, mesohaline, and polyhaline salinity eco-regions, respectively.

For example, in the oligohaline eco-region, salinity had a significant negative influence on total carbon only (Supplementary Fig. 9b). In the mesohaline eco-region, LAI was lower in areas of higher salinity (Supplementary Fig. 9c). However, in the polyhaline eco-region, salinity had an indirect negative influence on DBH (Supplementary Fig. 9d). Details about the non-significant and indirect associations are reported in Supplementary Fig. 9.

3.3. Power-law scaling to salinity modified functional variables

We found that salinity-driven ecosystem functional variables such as forest growth and carbon pools follow a power-law distribution (Fig. 7a-d, upper row). In addition, power-law fit curves denote functional variables decline consistently with increasing salinity (Fig. 7 e-h; $p < 0.01$).

4. Discussion

4.1. Salinity effects on mangrove forest structure, nutrients, functional traits, and functions

Our study found salinity to have multiple ecosystem consequences including the reduction of structural variables such as tree height, DBH, stand basal area, leaf area, nutrients, growth, productivity, etc. which supports our first hypothesis. We observed low nutrients (N, P, and K) in high saline areas (Fig. 2C a-c), which ultimately reduces site quality and makes the sites poor. This might happen due to limited microbial activities in high saline eco-regions as salinity restricts nutrient release by limiting microbial activities (Alongi, 2018). However, salinity impacts are more evident in salinity ecozones when considering the distribution of forest variables as high salinity reduced most of the forest variables (Fig. 2). We demonstrated strong evidence that several forest ecosystem functions are restricted under high salinity and low nutrient ecozone or sites (i.e., poor sites) (Figs. 2, 3). The finding of decreasing patterns of functional variables (growth and carbon pools) with increased salinity has also been evidenced by other studies conducted in various mangrove forests. For example, Banerjee et al. (2017) observed salinity reduced above ground biomass of *H. fomes* in the Indian Sundarbans.

Although salinity reduced the forest parameters such as height, DBH, etc. and site conditions, species diversity showed reverse patterns, meaning it increased with salinity, which is consistent with the findings of Sarker et al. (2019b). This might be explained by the analogous findings of co-occurrence of several high salt-tolerant species (i.e., *E. agallocha, C. decandra,* etc.) that occupied the higher salinity eco-regions. This species

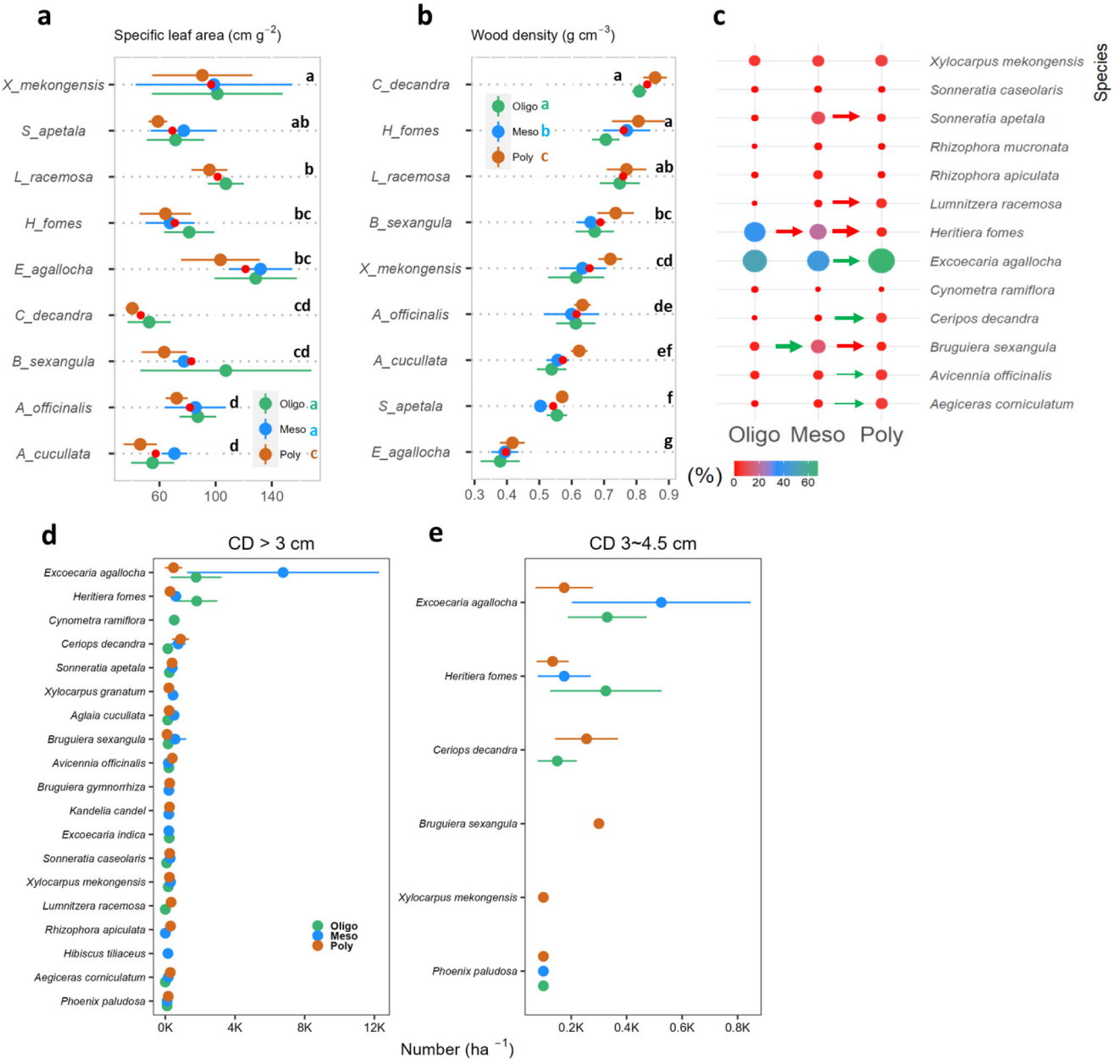

Fig. 4. Species-level variations in functional traits [(a) specific leaf area, (b) wood density], (c) tree-specific compositional percentage and regeneration success, [(d) mean seedling density (collar diameter, CD > 3 cm) and (e) mean seedling density (collar diameter 3– 4.5 cm)] across the salinity eco-regions. In subpanels a, b, d and e, green, blue and orange horizontal lines indicate the range (95 % confidence interval), and the circle denotes the mean values, while red point defining the mean values for specific species. Green arrows indicate an increasing trend, while red arrows indicate a decreasing trend in (c). Different letters are adopted from the post-hoc Tukey test. Similar letters denote no significant differences. Colored letters denote difference between zones, and black letters indicate differences between species.

patterns can also be linked with nutrient availability as nutrient can alter species distribution and their composition (Alongi, 2018). Additionally, we recorded that a few salt-intolerant species such as *H. fomes* largely disappeared from the high salinity and low nutrient areas which has already been evidenced by Sarker et al. (2016). They explained that *H. fomes* abundances decreased with increasing salinity, which may be making this forest more homogeneous (Sarker et al., 2019a) and affect the forest functions. Another study in the Indian Sundarbans observed that salinity restricted the distribution of several less salt-tolerant species including *H. fomes* and favored widespread colonization of generalist species such as *E. agallocha* (Chowdhury et al., 2019). We thus envisage that if the increasing salinity pattern continues, site quality will be declined (high salinity and low nutrients), and future canopy cover will be dominated by highly salt-tolerant generalist species such as *E. agallocha* or *C. decandra*. Our prediction could be supported by higher salt-tolerant seedling abundance in high saline areas, as we observed greater regeneration or seedlings of these species in higher salinity ecozones (Fig. 4d, e). This unequal species distribution across site gradients (variations in salinity and nutrients) might have a critical impact on tree functional traits such as leaf area.

Moreover, we observed that tree functional traits are highly responsive to site conditions such as salinity and nutrients. To illustrate, leaf area (LAI), specific leaf area (SLA, related to resource acquisition) of almost all species showed declining trend with salinity, while about all species showed a plastic enhancement of wood density (WD, resource conservation) with increasing salinity (Figs. 2D d1, 4a, b). We also identified strong influences of site quality on dominant height (Fig. 3e). Above mentioned functional variables are crucial as specific leaf area (SLA) and dominant height are growth-promoting features that describe the site condition and the plant's

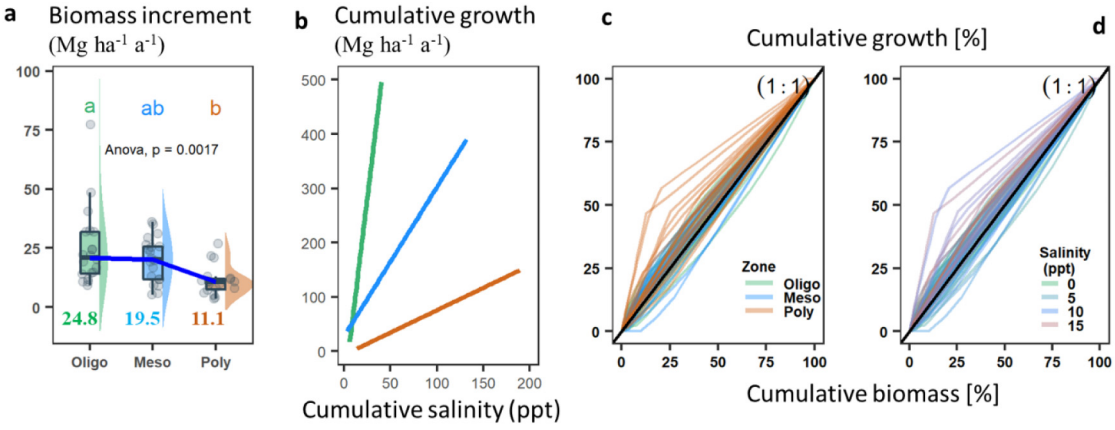

Fig. 5. Variations in growth and growth dominance (GD) patterns across the different salinity eco-regions and salinity gradients: (a) Variations in growth across salinity eco-regions; (b) cumulative growth patterns with cumulative salinity; (c) growth dominance patterns across the salinity eco-regions; and (d) growth dominance pattern across the salinity gradient. (c) and (d) were developed by arranging the values smallest to largest, as proposed by Binkley et al. (2006). Colored lines above the black solid straight lines (1:1) denote negative growth dominance, lines below the 1:1 solid line signify positive growth dominance, and identical lines 1:1 represent zero growth dominance. Different letters show significant differences, i.e., adopted from the Tukey Post hoc test. Blue solid line in (a) denotes the growth trend and values are shown in the inset. GD is defined as the tree growth distribution across tree sizes. For example, if large trees in a stand shared higher growth than biomass, indicating positive or strong GD (see more in Binkley et al. (2006)).

resource-acquisition strategy (Poorter et al., 2006; Tao et al., 2016). Height regulates the light acquisition ability (Poorter et al., 2006) while SLA reflects the light capture efficiency of the leaf (Perez-Harguindeguy et al., 2013), thereby regulating the plant's growth. In contrast, wood density (WD) largely controls plant architecture and growth (Putz et al., 1983). Species in the poor sites (high salinity and low nutrients) showed lower SLA, denoting less photosynthetic activity in poor site conditions and thereby lower growth. It further highlights that poor sites strongly modify functional traits (i.e., WD, SLA, etc.) and have a greater impact on ecosystem functions. Besides, trees in polyhaline eco-regions are largely exposed to the sea, which might have increased WD (plastic enhancement) to survive against strong winds. This exposing feature, i.e., being exposed to the sea,

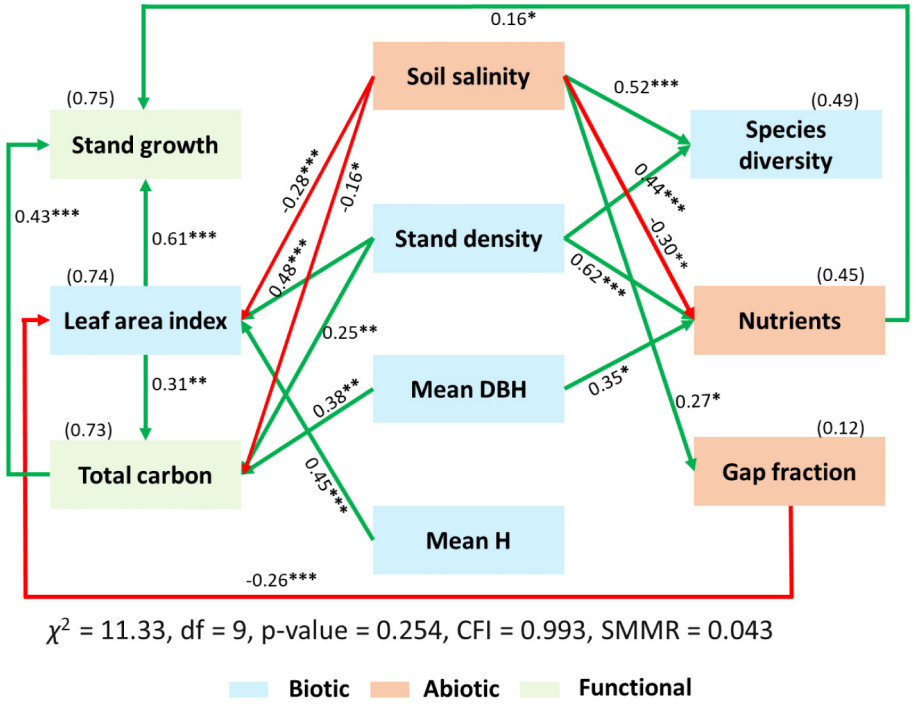

Fig. 6. Structural equation models (SEMs) showing the diverse associations with growth, total carbon pools (aboveground and belowground), and stand structures. (a) Developed SEM model goodness of fit tests, $\chi^2 = 11.33$, $p = 0.254$, with a comparative fit index (CFI) close to one (CFI = 0.99) (Bentler, 1990) and standardized root mean square residual (SMMR = 0.043) indicating had no significant deviation from model datasets at 9 degree of freedom. The green and red arrows indicate the pathways of positive and negative effects between covariates, respectively. Arrows with numbers indicate the standardized association of predictors with dependent variables. Numbers with the above boxes indicate their explained variance (coefficient of determinant: R^2 indicates the proportion of variance explained) by all the predictors. The adjacent path values indicate the standardized path coefficients indicated with their significance level (asterisk signs) (***$p < 0.001$; **$p < 0.01$; *$p < 0.05$). Only significant relationships are shown. Please see Supplementary Fig. 9 for non-significant and indirect relationships.

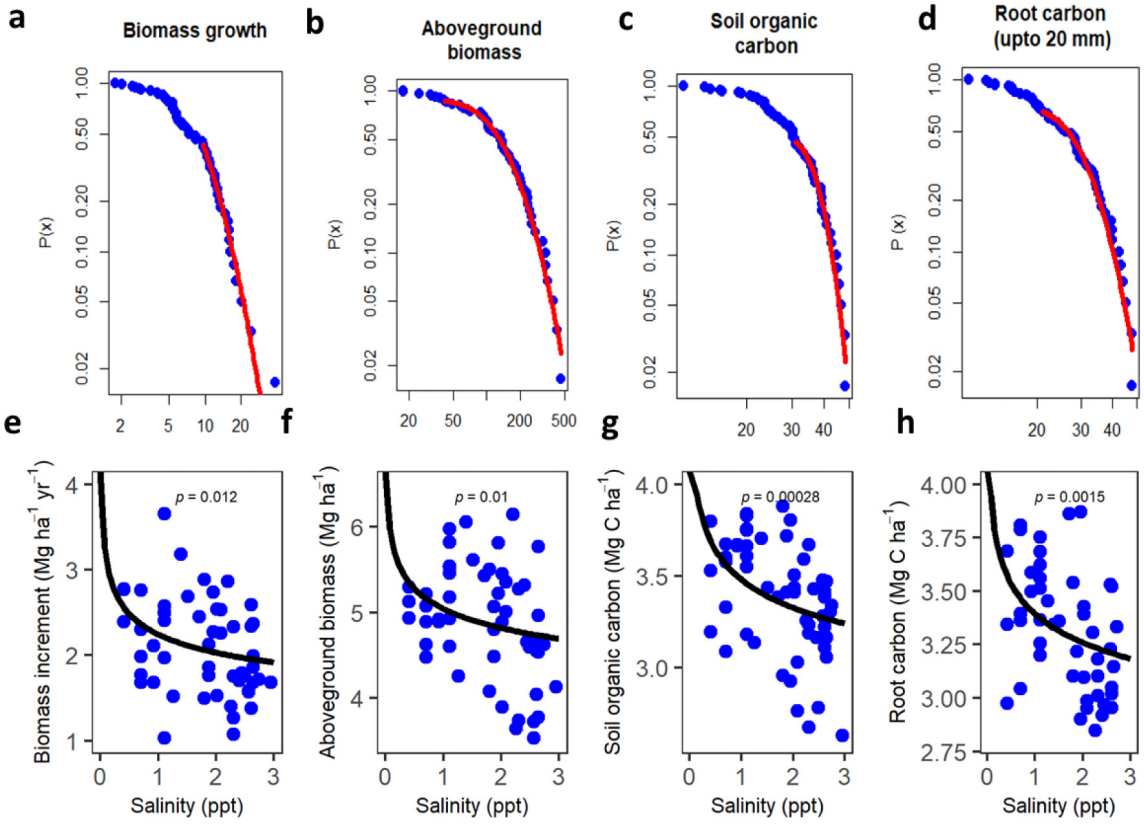

Fig. 7. Power law distributions of ecosystem functional variables. P(x) defines complementary cumulative distribution of functional variables (upper row, a-d) and red line fits power law with logarithmic line. Lower row denotes different functional variables and power law fits with salinity (e-h).

may have resulted in frequent inundation with saline water and forced the polyhaline mangrove region to act as a fringing mangrove (different from low saline forest areas as they are not directly exposed to the sea) (i.e., shown in Fig. 1). This critical factor could make the ecosystem (i.e., especially associated with high saline areas in SMF) more vulnerable and less productive, as described in Ward et al. (2016). These unfavorable conditions could also have enhanced tree mortality in poor site conditions and thereby the canopy gaps, as we observed higher gap fractions in the polyhaline zone (Fig. 3i). However, we were unable to quantify the inundation effect on ecosystem functions and its role in creating canopy gaps. Therefore, future research should focus on how inundation frequency and durability effects affect mangrove ecosystems functions and functionality.

With increasing salinity and lowering nutrients, we found WD in almost all species increased, while Rahman et al. (2021a) discussed that salinity lowered plot level WD, which is contradictory to our species-level study. They further observed salinity lowered the canopy height at stand level, which is identical to our study as we also observed sites with high salinity and low nutrients reduced the height and dominant height of trees (top 20 % of trees) (Figs. 2A a4, a6; 3e, f), denoting the relative restrictiveness of salinity and salinity-driven poor sites from stand to individual tree level. Our results were further compared with Sarker et al. (2021), who found increasing salinity reduced the LAI, SLA, and increased WD of mangroves, although different species showed different responses towards salinity. This diverse response of functional traits to salinity observed in different studies could be occurred due to species sampled and site quality variations in the study sites. This spatial variability can also be linked with geomorphic and local environmental settings (e.g., stand to plot-level salinity and nutrient variations) as the local environmental setting (nutrient availability) can determine species and biomass distribution (Castañeda-Moya et al., 2013; Simard et al., 2019), thereafter functional traits. In addition, a species' functional distinctiveness might have a significant impact on functional traits (Rahman et al., 2021a). Here, we observed the tallest mangrove, species with low wood density, and high growth rate in a low salinity ecozone, indicating the site conditions and local environmental setting largely explain the mangrove species' attributes and functions. Besides, the high carbon stocks (both above and below ground) were recorded in the low saline ecozone. This could be the result of higher nutrients such as N, P, and K availability (Fig. 2C) and nutrient-induced higher species growth (Fig. 5a, b). These nutrients and their spatial variability could also be influenced by the species, stand structure (such as height, DBH), and their functions (Simard et al., 2019).

Furthermore, we observed a higher growth rate in the oligohaline zone (Fig. 5a), which is supplemented by the cumulative growth curve, as the higher the soil salinity, the flatter the growth curve (Fig. 5b). This is further relatable to mangroves in Myanmar, where Win et al. (2019) found that soil salinity along with tidal inundation restricted mangrove growth rates. In addition, growth dominance patterns observed in higher salinity zones are quite distinctive from growth pattern in oligohaline or less saline zone. We identified negative growth dominance patterns in higher saline eco-regions (Fig. 5c, d), denoting larger tree growth was limited with smaller trees having greater contributions to growth than biomass, which can be explained by higher competition (Binkley, 2004; Binkley et al., 2006). Negative GD patterns indicated that growth partitioning favored small trees in high saline areas. On the contrary, trees in comparatively lower saline regions mostly displayed positive growth dominance (Fig. 5c, d), denoting minimal competition and suggesting growth partitioning shifted towards large trees. These GD patterns might be connected with the variation in site conditions (low nutrient, high salinity vs. high nutrient, low salinity). In rich sites (high nutrient, low salinity), large trees may get an over proportionate benefit (i.e., benefit of dominance) from their size, but in poor sites (low nutrient, high salinity), they may not do so as we observed large trees are losing growth due to higher magnitude of salinity (see GD patterns in Fig. 5c-d). These diverse GD patterns indicate higher structural diversity in rich sites (Binkley et al.,

2006). An analogous finding, we observed in fewer saline or rich site areas to demonstrate high DBH, height, and their variations (high nutrient and low salinity) (Fig. 2A a1-a6; C c1-c3). Also, a continuous increase in salinity patterns may not affect the growth of small trees but limit the growth of large trees. This may suggest that the large trees are more saline sensitive and may lose functions (e.g. growth) more rapidly than smaller trees, implying that the biomass accumulation rate may be slowed with rapid salinity changes when growth partitioning is skewed towards small trees. This finding might be applicable for other mangroves growing in different parts (i.e., where salinity is a major concern) of the world with future global climate change.

4.2. Linking functional variables with biotic and abiotic factors

This study identified that biotic and abiotic factors critically influence forest functions and growth dynamics either directly or indirectly and individually or combinedly. To illustrate, salinity and salinity-driven canopy gaps (evaluated through gap fraction) have a direct negative influence on carbon stocks, nutrients, and LAI but no direct impact on growth but indirectly affect growth by limiting LAI and nutrients (Fig. 6). We expected species diversity could have a direct influence on functional variables such as growth or carbon stocks, but SEM depicted no direct significant influence on forest functions (Fig. 6; also see Supplementary Fig. 9). In contrast, previous studies claimed a positive influence of higher species richness on carbon stocks (Rahman et al., 2021a), but we were unable to detect any significant effect of species richness or diversity on forest functional variables, which leads to partial support for our second hypothesis. The influence on growth and biomass or carbon stocks may be species and geographic-specific. For example, high numbers of *H. fomes* could largely affect the growth in a less saline zone but the abundance of salt-tolerant dwarf species in high saline areas might decline the forest growth. Another reason could be soil conditions; as high salinity along with low nutrients (Supplementary Fig. 10) makes the soil more anaerobic, resulting in poor forest growth and declining species-specific forest structure, thereby lower carbon pools in the high salinity eco-region in the Bangladesh Sundarbans. As earlier studies reported that forest growth and forest structure in mangroves are controlled by site gradients (for example, nutrient availability and salinity) (Twilley and Rivera-Monroy, 2009). In consistence with that notion, our study demonstrated that forest growth was largely determined by nutrients (N, P, and K), salinity, and stand structure (such as height, DBH, leaf area, tree density, etc.) (Figs. 3a, 5, Supplementary Fig. 8). This relationship was also identified by the SEM model (Fig. 6, Supplementary Fig. 9). Chowdhury et al. (2019) reported similar findings for the Indian part of the Sundarbans illustrating soil with poor nutrients and higher salinity negatively modified forest structure and reduced forest coverage from 98 % to 10 %. Here, we acknowledge that apart from salinity, geomorphic and hydrological features (e.g., river bank erosion, landforms, inundation duration, frequency and height, etc.) could also play important roles in shaping mangrove structure and functions. Therefore, we recommend for including important geomorphological and hydroperiod data as predictors in future SEM model as these data become available.

Besides, faster tree growth adds more aboveground biomass (Temmerman et al., 2012), whereas SEM identified their (i.e., biomass or carbon stocks and growth) direct linkage, denoting higher tree growth adding more biomass and carbon to the ecosystem in this mangrove forest. Furthermore, organic carbon is a well-recognized soil fertility indicator (Begam et al., 2020), and high salinity or poor sites may be working against SOC accumulation in the mangrove soil (Kida et al., 2017). SOC is also linked with forest growth, as higher biomass growth specifically root growth contributes to soil carbon in soil substrate (Rogers et al., 2019). We observed higher growth and soil carbon in less saline eco-regions (Figs. 2B b4 and 5a, b), while both are positively associated with each other, evidenced by the SEM model (Fig. 6 and Supplementary Fig. 9a). This may indicate that forest growth contributes soil carbon through producing roots and their decomposition or vice versa. However, high salinity and low nutrients might reverse this relationship from positive to negative in high saline regions (Supplementary Fig. 9d), as low biomass growth and carbon stocks in polyhaline areas were observed. However, we could not explain how salinity influences the load of allochthonous and autochthonous organic matter input into the Sundarbans due to data scarcity, thus suggesting the need for new studies on this. In addition, we found higher aboveground carbon than belowground soil carbon stocks (Fig. 2B b2-b3), similar results reported in the previous study by Rahman et al. (2021b), where they also found low soil organic carbon than aboveground carbon. This could have happened due to sampling depth (only 50 cm in our case) and stand age (young type of forest as DBH distribution showed a reserve J shape curve, see Supplementary Fig. 5) as with stand age soil carbon stocks increase (Adame et al., 2013). Low soil carbon burial could be another reason for low SOC in high saline areas, as sea-level rise reduces decomposition by increasing salinity, thereby influencing soil carbon burial (Spivak et al., 2019). Thus, we can conclude that mangrove forest functions largely depend on site quality (nutrients and salinity) and associated stands, i.e., species compositions and their structure, although the overall site and stand structure depend on the magnitude of salinity stress.

4.3. Power-law scaling to functional variables

We found, in support of our hypothesis three, that the salinity-driven functional variables can be generalizable by the power-law. We observed forest ecosystem functions disproportionately declined with rapid changes in salinity and followed the power-law distribution (Fig. 7). Although our overarching hypothesis was that data from high salinity eco-regions may only support the power law as functional variable distributions well fitted with lower distribution data (Fig. 7a-d), this could be varied from the global dataset but may also be consistent with our finding. We expect a universal power-law relationship exists between salinity and forest functions across mangrove forests around the world, specifically where salinity is the most restrictive factor. However, this study only evaluated power-law behaviors to salinity and functional variable relationships (as salinity is the recognized restricting forest variable), but future studies would be interesting if they added nutrient and site quality to power-law scaling.

4.4. Implications for forest management and future directions

Due to rapid changes in the climate, sea-level rise has been projected to increase and is considered a major threat to mangrove ecosystems worldwide (Ward et al., 2016). The projected sea-level rise in the Sundarbans (which is highest on the Indian coast compared to the global projection) (Karim and Mimura, 2008; Trivedi et al., 2016), and its severity especially on the plant community (Rahman, 2020) denotes Sundarbans will likely face adverse sea-level rise pointing to more salinity effects in the future. This may increase mortality leading to an increase in the forest gap and changes in the forest structure. If the sea-level rising pattern continues, inundation periods with high saline water will be prolonged as the Sundarbans mangrove forest is situated at the interface of land and sea and active delta (Mukhopadhyay et al., 2018). Hence, we hypothesized that inundation could be permanent all year long, not only in the Sundarbans mangrove forest but also in mangrove forests throughout the world due to remaining at the interface of land and sea. This will radically affect the mangrove forest's structure and ecosystem functioning at both regional and global levels which may further reduce the sequestering capability of highly productive mangrove forests. As discussed in the "Introduction" section, declining upstream water discharge enhances soil salinity. Therefore, maintaining freshwater discharge may be beneficial to reducing salinity and preserving less salt-tolerant species such as *H. fomes* and their compositions. This may again aid in maintaining the overall ecosystem functions, necessitating strong policy implications.

In addition, to avoid the functional collapse of mangroves, restoring the habitats of threatened species such as *H. fomes* in forest gaps that occurred due to salinity-induced fragmentation (as we observed a higher gap in high salinity ecozone) (see Figs. 2 Dd2 and 3i) could be an efficient way of

minimizing the impacts of salinity. However, we need comprehensive baseline information related to restoration feasibility (cost- benefit analysis), particularly species and site selections (Dasgupta et al., 2019; Rahman and Mahmud, 2018; Saenger and Siddiqi, 1993). Thus, we propose to compile a comprehensive database for a better understanding the power-law scaling behavior and MST predictions to mangrove tree size and shape including forest functions at a global level. This global understanding is critical as trees tree structure (i.e., shape and size) largely impacted by growing condition (Jucker et al., 2015).

Besides, our fitted power-law distributions expressed consistent and proportional decline of functional variables with rising salinity. Future analysis could test the power law in climate-driven functional variables in diverse mangrove forests. This is despite the fact that we tested the power-law pattern with limited datasets, such as data from only 60 permanent plots. But our initial results could be supplemented with the universality of power-law distributions and relationships between salinity and forest functional variables in natural and planted mangroves to generalize the concept, gaining global attention. However, this study produces a unique dataset comprising, fine-scale species, habitat, functional traits, and growth data. This offers the opportunity for others to build on this dataset, collect new data to test different ecological hypotheses (that we couldn't *t*-test here such as verifying the power-law universality in climate-driven functional variables in different mangrove forests throughout the world), and may also help to develop mechanistic models for projecting mangrove structure and functions under changes in a local environment and global changes in climate. We are expecting a critical understanding of complex ecological patterns that will expand our knowledge to incorporate silvicultural practice and help us better manage the mangrove forest to promote adaptability to climate change (Fahey et al., 2018).

5. Conclusions

This study revealed that salinity negatively shapes the forest by limiting the stand structure, ecosystem functional variables such as growth and carbon pools, and nutrient availability. In addition, functional traits such as specific leaf area declined while wood density increased with rapid salinity change for all observed species which denotes salinity affecting tree to community-level functions. Salinity modified variables showed different types of associations (i.e., positive or negative and direct or indirect) across salinity eco-regions. Furthermore, salinity-driven ecosystem functional variables tightly followed the power-law distribution, revealing that functional variables declined consistently and proportionately with a rapid change in salinity. This study demonstrated salinity as a strong restrictive factor that shrinks the mangrove forest ecosystems and their associated functions. This trend will further lead to less productive ecosystems with dwarf species and a reduced ability to sink more carbon. Our comprehensive findings suggest that maintaining low salinity may improve the ecological stability of the mangrove ecosystem in the face of climate change by buffering the influence of salinity. Almost all forest variables performed better in low salinity eco-regions than in high salinity areas. However, we still lack proper documentation of the prolonged inundation effects on mangrove ecosystems, which needs to be understood. Our findings have great implications for forest management decision-making to conserve and maintain the unique mangrove ecosystems in Bangladesh. This comprehensive information can also be complemented and useful for understanding the growth patterns, ecosystem functioning, and conservation of global mangroves under future climate change.

Funding

The Commonwealth Scholarship Commission, UK (funding number: BDCA-2013-6), SUST Research Centre (Project Id: FES/2020/2/01), the Japan Society for the Promotion of Science (JSPS) (Reference: KAKENHI 15F15389), and the Grant-in-Aid for Scientific Research from Research Cell, Khulna University, Khulna-9208, Bangladesh have all contributed to this work.

This research is also supported by the European Union's Horizon 2020 research and innovation program under Marie Sklodowska-Curie Grant Agreement No. H2020-MSCA-ITN-2020-956355.

CRediT authorship contribution statement

Conceptualization-SA (lead), SKS. Data Collection- SKS (lead), SA, MK, MAI, TD. Formal analysis- SA (lead), MJS, MJ. Manuscript writing- SA (lead), SKS, MNHS, MAA. Review and Editing- HP (lead), DAF and MJ, CSSN, MAA. Final review- DAF, HP, and CSSN. All authors read and approved the final version of the manuscript.

Data availability

Data is shared with the manuscript and will be made available with the online version of the paper

Declaration of competing interest

The authors declare no competing interest.

Acknowledgements

We are grateful to the Bangladesh Forest Department for assisting us with logistics and allowing us to set up permanent sample sites as well as share salinity data. We also like to thank the Khulna Branch of the Bangladesh Meteorological Department for sharing rainfall, temperature, and humidity data with us. We also appreciate Dr. Mizanur Rahman's assistance and recommendations during the data analysis. We also like to express our gratitude to Dr. Peter Biber and Ms. Julia Schmucker, Chair of Forest Growth and Yield Science, School of Life Science Systems, Technical University of Munich, Germany, who assisted us with data analysis using R. Our sincere gratitude goes out to our study assistants, Forestry and Wood Technology Discipline, Khulna University, Bangladesh, who assisted with data collecting.

Appendix A. Supplementary data

Supplementary data to this article can be found online at https://doi.org/10.1016/j.scitotenv.2022.158662.

References

Abdullah, A.N.M., Stacey, N., Garnett, S.T., Myers, B., 2016. Economic dependence on mangrove forest resources for livelihoods in the Sundarbans, Bangladesh. Forest Policy Econ. 64, 15–24.

Adame, M.F., Kauffman, J.B., Medina, I., Gamboa, J.N., Torres, O., Caamal, J.P., et al., 2013. Carbon stocks of tropical coastal wetlands within the karstic landscape of the Mexican Caribbean. PloS one 8, e56569.

Addo-Danso, S.D., Prescott, C.E., Smith, A.R., 2016. Methods for estimating root biomass and production in forest and woodland ecosystem carbon studies: a review. For. Ecol. Manag. 359, 332–351.

Ahmed, I., Iqbal, Z., 2011. Sundarbans carbon inventory (2010) a comparison with 1997 inventory. SAARC For. J. 1, 59–72.

Ahmed, S., Kamruzzaman, M., 2021. Species-specific biomass and carbon flux in Sundarbans mangrove forest, Bangladesh: response to stand and weather variables. Biomass Bioenergy 153, 106215.

Ahmed, S., Kamruzzaman, M., Azad, M.S., Khan, M.N.I., 2021. Fine root biomass and its contribution to the mangrove communities in three saline zones of Sundarbans, Bangladesh. Rhizosphere 17, 100294.

Alongi, D.M., 2018. Impact of global change on nutrient dynamics in mangrove forests. Forests 9, 596.

Alongi, D.M., 2022. Impacts of climate change on blue carbon stocks and fluxes in mangrove forests. Forests 13, 149.

Aziz, A., Paul, A.R., 2015. Bangladesh Sundarbans: present status of the environment and biota. Diversity 7, 242–269.

Banerjee, K., Gatti, R.C., Mitra, A., 2017. Climate change-induced salinity variation impacts on a stenoecious mangrove species in the Indian Sundarbans. Ambio 46, 492–499.

Begam, M.M., Chowdhury, R., Sutradhar, T., Mukherjee, C., Chatterjee, K., Basak, S.K., et al., 2020. Forecasting mangrove ecosystem degradation utilizing quantifiable ecophysiological resilience-a study from Indian Sundarbans. Sci. Rep. 10, 1–14.

Bentler, P.M., 1990. Comparative fit indexes in structural models. Psychol. Bull. 107, 238.

Binkley, D., 2004. A hypothesis about the interaction of tree dominance and stand production through stand development. For. Ecol. Manag. 190, 265–271.
Binkley, D., Kashian, D.M., Boyden, S., Kaye, M.W., Bradford, J.B., Arthur, M.A., et al., 2006. Patterns of growth dominance in forests of the Rocky Mountains, USA. For. Ecol. Manag. 236, 193–201.
Bremner, J.M., Breitenbeck, G.A., 1983. A simple method for determination of ammonium in semimicro-kjeldahl analysis of soils and plant materials using a block digester. Commun. Soil Sci. Plant Anal. 14, 905–913.
Carugati, L., Gatto, B., Rastelli, E., Martire, M.L., Coral, C., Greco, S., et al., 2018. Impact of mangrove forests degradation on biodiversity and ecosystem functioning. Sci. Rep. 8, 1–11.
Castañeda-Moya, E., Twilley, R.R., Rivera-Monroy, V.H., Marx, B.D., Coronado-Molina, C., Ewe, S.M.L., 2011. Patterns of root dynamics in mangrove forests along environmental gradients in the Florida Coastal Everglades, USA. Ecosystems 14, 1178–1195.
Castañeda-Moya, E., Twilley, R.R., Rivera-Monroy, V.H., 2013. Allocation of biomass and net primary productivity of mangrove forests along environmental gradients in the Florida Coastal Everglades, USA. For. Ecol. Manag. 307, 226–241.
Chave, J., et al., 2009. Towards a worldwide wood economics spectrum. Ecol. Lett. 12, 351–366. https://doi.org/10.1111/j.1461-0248.2009.01285.x.
Chen, L., Wang, W., 2017. Ecophysiological responses of viviparous mangrove Rhizophora stylosa seedlings to simulated sea-level rise. J. Coast. Res. 33, 1333–1340.
Chowdhury, R., Sutradhar, T., Begam, M., Mukherjee, C., Chatterjee, K., Basak, S.K., et al., 2019. Effects of nutrient limitation, salinity increase, and associated stressors on mangrove forest cover, structure, and zonation across Indian Sundarbans. Hydrobiologia 842, 191–217.
Conti, G., Díaz, S., 2013. Plant functional diversity and carbon storage–an empirical test in semi-arid forest ecosystems. J. Ecol. 101, 18–28.
Damptey, F.G., Birkhofer, K., Oliveras Menor, I., de la Riva, E.G., 2022. The functional structure of tropical plant communities and soil properties enhance ecosystem functioning and multifunctionality in different ecosystems in Ghana. Forests 13.
Dasgupta, S., Islam, M.S., Huq, M., Huque Khan, Z., Hasib, M.R., 2019. Quantifying the protective capacity of mangroves from storm surges in coastal Bangladesh. PloS one 14, e0214079.
Donato, D.C., Kauffman, J.B., Murdiyarso, D., Kurnianto, S., Stidham, M., Kanninen, M., 2011. Mangroves among the most carbon-rich forests in the tropics. Nat. Geosci. 4, 293–297.
Duncanson, L., Rourke, O., Dubayah, R., 2015. Small sample sizes yield biased allometric equations in temperate forests. Sci. Rep. 5, 1–13.
Ellison, J.C., 2015. Vulnerability assessment of mangroves to climate change and sea-level rise impacts. Wetl. Ecol. Manag. 23, 115–137.
Fahey, R.T., Alveshere, B.C., Burton, J.I., D'Amato, A.W., Dickinson, Y.L., Keeton, W.S., et al., 2018. Shifting conceptions of complexity in forest management and silviculture. For. Ecol. Manag. 421, 59–71.
Farrior, C.E., Bohlman, S.A., Hubbell, S., Pacala, S.W., 2016. Dominance of the suppressed: power-law size structure in tropical forests. Science 351, 155–157.
Friess, D.A., 2019. Where the tallest mangroves are. Nat. Geosci. 12, 4–5.
Friess, D.A., Rogers, K., Lovelock, C.E., Krauss, K.W., Hamilton, S.E., Lee, S.Y., et al., 2019. The state of the world's mangrove forests: past, present, and future. Annu. Rev. Environ. Resour. 44, 89–115.
Friess, D.A., Yando, E.S., Alemu, J.B., Wong, L.-W., Soto, S.D., Bhatia, N., 2020. Ecosystem services and disservices of mangrove forests and salt marshes. Oceanogr. Mar. Biol. 58, 107–142.
Gee, G.W., Bauder, J.W., 1986. Particle-size analysis 1. Methods of soil analysis: part 1—physical and mineralogical methods. Agron. Monogr. 9.
Gifford, R.M., 2000. Carbon Contents of Above-ground Tissues of Forest and Woodland Trees. Australian Greenhouse Office.
Gillespie, C.S., 2014. Fitting heavy tailed distributions: the poweRlaw package arXiv preprint arXiv:1407.3492.
Giri, C., Ochieng, E., Tieszen, L.L., Zhu, Z., Singh, A., Loveland, T., et al., 2011. Status and distribution of mangrove forests of the world using earth observation satellite data. Glob. Ecol. Biogeogr. 20, 154–159.
Goldberg, L., Lagomasino, D., Thomas, N., Fatoyinbo, T., 2020. Global declines in human-driven mangrove loss. Glob. Chang. Biol. 26, 5844–5855.
Grace, J.B., Schoolmaster Jr., D.R., Guntenspergen, G.R., Little, A.M., Mitchell, B.R., Miller, K.M., et al., 2012. Guidelines for a graph-theoretic implementation of structural equation modeling. Ecosphere 3, 1–44.
Halder, N.K., Merchant, A., Misbahuzzaman, K., Wagner, S., Mukul, S.A., 2021. Why some trees are more vulnerable during catastrophic cyclone events in the Sundarbans mangrove forest of Bangladesh? For. Ecol. Manag. 490, 119117.
Hamilton, S.E., Casey, D., 2016. Creation of a high spatio-temporal resolution global database of continuous mangrove forest cover for the 21st century (CGMFC-21). Glob. Ecol. Biogeogr. 25, 729–738.
Hortal, J., Borges, P.A.V., Jiménez-Valverde, A., de Azevedo, E.B., Silva, L., 2010. Assessing the areas under risk of invasion within islands through potential distribution modelling: the case of Pittosporum undulatum in São Miguel, Azores. J. Nat. Conserv. 18, 247–257.
Howard, J., Hoyt, S., Isensee, K., Telszewski, M., Pidgeon, E., 2014. Coastal Blue Carbon: Methods for Assessing Carbon Stocks and Emissions Factors in Mangroves, Tidal Salt Marshes, and Seagrasses.
Huang, Y., Chen, Y., Castro-Izaguirre, N., Baruffol, M., Brezzi, M., Lang, A., et al., 2018. Impacts of species richness on productivity in a large-scale subtropical forest experiment. Science 362, 80–83.
Iftekhar, M.S., Saenger, P., 2008. Vegetation dynamics in the Bangladesh Sundarbans mangroves: a review of forest inventories. Wetl. Ecol. Manag. 16, 291–312.
Islam, M.S., 2001. Sea-level Changes in Bangladesh: The Last Ten Thousand Years. Asiatic Society of Bangladesh.
Islam, S.N., Gnauck, A., 2009. Threats to the Sundarbans mangrove wetland ecosystems from transboundary water allocation in the Ganges basin: a preliminary problem analysis. Int. J.Ecol.Econ.Stat. 13, 64–78.
IWM, 2003. Sundarban Biodiversity Conservation Project. 1.
Jost, L., 2006. Entropy and diversity. Oikos 113, 363–375.
Jucker, T., Bouriaud, O., Coomes, D.A., 2015. Crown plasticity enables trees to optimize canopy packing in mixed-species forests. Funct. Ecol. 29, 1078–1086.
Jucker, T., Fischer, F.J., Chave, J., Coomes, D.A., Caspersen, J., Ali, A., et al., 2022. Tallo–a global tree allometry and crown architecture database. Glob. Chang. Biol. 28, 5254–5268.
Kamruzzaman, M., Ahmed, S., Osawa, A., 2017. Biomass and net primary productivity of mangrove communities along the oligohaline zone of Sundarbans, Bangladesh. For. Ecosyst. 4, 1–9.
Karim, M.F., Mimura, N., 2008. Impacts of climate change and sea-level rise on cyclonic storm surge floods in Bangladesh. Glob. Environ. Chang. 18, 490–500.
Kida, M., Tomotsune, M., Iimura, Y., Kinjo, K., Ohtsuka, T., Fujitake, N., 2017. High salinity leads to accumulation of soil organic carbon in mangrove soil. Chemosphere 177, 51–55.
Kirwan, M.L., Megonigal, J.P., 2013. Tidal wetland stability in the face of human impacts and sea-level rise. Nature 504, 53–60.
Komiyama, A., Ogino, K., Aksornkoae, S., Sabhasri, S., 1987. Root biomass of a mangrove forest in southern Thailand. 1. Estimation by the trench method and the zonal structure of root biomass. J. Trop. Ecol. 3, 97–108.
LaRue, E.A., Hardiman, B.S., Elliott, J.M., Fei, S., 2019. Structural diversity as a predictor of ecosystem function. Environ. Res. Lett. 14, 114011.
Lasky, J.R., et al., 2014. Trait-mediated assembly processes predict successional changes in community diversity of tropical forests. Proc. Natl. Acad. Sci. 111, 5616–5621. https://doi.org/10.1073/pnas.1319342111.
Lawson, J.R., et al., 2015. Hydrological conditions explain variation in wood density in riparian plants of south-eastern Australia. J. Ecol. 103, 945–956. https://doi.org/10.1111/1365-2745.12408.
Lee, C.K.F., Duncan, C., Nicholson, E., Fatoyinbo, T.E., Lagomasino, D., Thomas, N., et al., 2021. Mapping the extent of mangrove ecosystem degradation by integrating an ecological conceptual model with satellite data. Remote Sens. 13, 2047.
Liu, X., Trogisch, S., He, J.-S., Niklaus, P.A., Bruelheide, H., Tang, Z., et al., 2018. Tree species richness increases ecosystem carbon storage in subtropical forests. Proc. R. Soc. B 285, 20181240.
Moles, A.T., et al., 2009. Global patterns in plant height. J. Ecol. 97, 923–932. https://doi.org/10.1111/j.1365-2745.2009.01526.x.
Mörner, N.-A., 2010. Sea level changes in Bangladesh new observational facts. Energy Environ. 21, 235–249.
Mukhopadhyay, A., Wheeler, D., Dasgupta, S., Dey, A., Sobhan, I., 2018. Aquatic Salinization and Mangrove Species in a Changing Climate.
Nicotra, A.B., et al., 2010. Plant phenotypic plasticity in a changing climate. Trends Plant Sci. 15, 684–692. https://doi.org/10.1016/j.tplants.2010.09.008.
Perez-Harguindeguy, N., Diaz, S., Garnier, E., Lavorel, S., Poorter, H., Jaureguiberry, P., et al., 2013. New handbook for standardised measurement of plant functional traits worldwide. Aust. Bot. 61, 167–234.
Peters, R., Walther, M., Lovelock, C., Jiang, J., Berger, U., 2020. The interplay between vegetation and water in mangroves: new perspectives for mangrove stand modelling and ecological research. Wetl. Ecol. Manag. 28, 697–712.
Poorter, L., et al., 2010. The importance of wood traits and hydraulic conductance for the performance and life history strategies of 42 rainforest tree species. New Phytol. 185, 481–492. https://doi.org/10.1111/j.1469-8137.2009.03092.x.
Poorter, L., Bongers, L., Bongers, F., 2006. Architecture of 54 moist-forest tree species: traits, trade-offs, and functional groups. Ecology 87, 1289–1301.
Putz, F.E., Coley, P.D., Lu, K., Montalvo, A., Aiello, A., 1983. Uprooting and snapping of trees: structural determinants and ecological consequences. Can. J. For. Res. 13, 1011–1020.
Rahman, M.M., 2020. Impact of increased salinity on the plant community of the Sundarbans Mangrove of Bangladesh. Community Ecol. 21, 273–284.
Rahman, M.R., Begum, S., 2011. Land cover change analysis around the Sundarbans Mangrove Forest of Bangladesh using remote sensing and GIS application. J.Sci.Found. 9, 95–107.
Rahman, M.M., Mahmud, M.A., 2018. Economic feasibility of mangrove restoration in the Southeastern Coast of Bangladesh. Ocean Coast.Manag. 161, 211–221.
Rahman, M., Nabiul Islam Khan, M., Fazlul Hoque, A.K., Ahmed, I., 2015. Carbon stock in the Sundarbans mangrove forest: spatial variations in vegetation types and salinity zones. Wetl. Ecol. Manag. 23, 269–283.
Rahman, M.M., Zimmer, M., Ahmed, I., Donato, D., Kanzaki, M., Xu, M., 2021a. Co-benefits of protecting mangroves for biodiversity conservation and carbon storage. Nat. Commun. 12, 1–9.
Rahman, M.S., Donoghue, D.N.M., Bracken, L.J., 2021b. Is soil organic carbon underestimated in the largest mangrove forest ecosystems?Evidence from the Bangladesh Sundarbans. Catena 200, 105159.
Rahman, M.S., Donoghue, D.N.M., Bracken, L.J., Mahmood, H., 2021c. Biomass estimation in mangrove forests: a comparison of allometric models incorporating species and structural information. Environ. Res. Lett. 16, 124002.
Ratcliffe, S., Wirth, C., Jucker, T., van der Plas, F., Scherer-Lorenzen, M., Verheyen, K., et al., 2017. Biodiversity and ecosystem functioning relations in european forests depend on environmental context. Ecol. Lett. 20, 1414–1426.
Ray, R., Michaud, E., Aller, R.C., Vantrepotte, V., Gleixner, G., Walcker, R., et al., 2018. The sources and distribution of carbon (DOC, POC, DIC) in a mangrove dominated estuary (French Guiana, South America). Biogeochemistry 138, 297–321.
Reef, R., Feller, I.C., Lovelock, C.E., 2010. Nutrition of mangroves. Tree Physiol. 30, 1148–1160.
Richards, D.R., Friess, D.A., 2016. Rates and drivers of mangrove deforestation in Southeast Asia, 2000–2012. Proc. Natl. Acad. Sci. 113, 344–349.
Rogers, K., Kelleway, J.J., Saintilan, N., Megonigal, J.P., Adams, J.B., Holmquist, J.R., et al., 2019. Wetland carbon storage controlled by millennial-scale variation in relative sea-level rise. Nature 567, 91–95.

Rosseel, Y., 2012. Lavaan: an R package for structural equation modeling. J. Stat. Softw. 48, 1–36.
Saenger, P., Siddiqi, N.A., 1993. Land from the sea: the mangrove afforestation program of Bangladesh. Ocean Coast.Manag. 20, 23–39.
Sarker, S.K., 2017. Spatial and Temporal Patterns of Mangrove Abundance, Diversity and Functions in the Sundarbans.
Sarker, S.K., Reeve, R., Thompson, J., Paul, N.K., Matthiopoulos, J., 2016. Are we failing to protect threatened mangroves in the Sundarbans world heritage ecosystem? Sci. Rep. 6, 1–12.
Sarker, S.K., Matthiopoulos, J., Mitchell, S.N., Ahmed, Z.U., Al Mamun, M.B., Reeve, R., 2019a. 1980s–2010s: the world's largest mangrove ecosystem is becoming homogeneous. Biol. Conserv. 236, 79–91.
Sarker, S.K., Reeve, R., Paul, N.K., Matthiopoulos, J., 2019b. Modelling spatial biodiversity in the world's largest mangrove ecosystem—the Bangladesh Sundarbans: a baseline for conservation. Divers. Distrib. 25, 729–742.
Sarker, S.K., Reeve, R., Matthiopoulos, J., 2021. Solving the fourth-corner problem: forecasting ecosystem primary production from spatial multispecies trait-based models. Ecol. Monogr. 91, e01454.
Shenkin, A., Bentley, L.P., Oliveras, I., Salinas, N., Adu-Bredu, S., Marimon-Junior, B.H., et al., 2020. The influence of ecosystem and phylogeny on tropical tree crown size and shape. Front.For.Glob.Chang. 3, 109.
Simard, M., Fatoyinbo, L., Smetanka, C., Rivera-Monroy, V.H., Castañeda-Moya, E., Thomas, N., et al., 2019. Mangrove canopy height globally related to precipitation, temperature and cyclone frequency. Nat. Geosci. 12, 40–45.
Spivak, A.C., Sanderman, J., Bowen, J.L., Canuel, E.A., Hopkinson, C.S., 2019. Global-change controls on soil-carbon accumulation and loss in coastal vegetated ecosystems. Nat. Geosci. 12, 685–692.
Tao, S., Guo, Q., Li, C., Wang, Z., Fang, J., 2016. Global patterns and determinants of forest canopy height. Ecology 97, 3265–3270.
Temmerman, S., Moonen, P., Schoelynck, J., Govers, G., Bouma, T.J., 2012. Impact of vegetation die-off on spatial flow patterns over a tidal marsh. Geophys. Res. Lett. 39.
The_World_Bank, 2022. Increasing Salinity in a Changing Climate Likely to Alter Sundarban's Ecosystem. 2017.
Thomas, N., Lucas, R., Bunting, P., Hardy, A., Rosenqvist, A., Simard, M., 2017. Distribution and drivers of global mangrove forest change, 1996–2010. PloS one 12, e0179302.
Tilman, D., Lehman, C.L., Thomson, K.T., 1997. Plant diversity and ecosystem productivity: theoretical considerations. Proc. Natl. Acad. Sci. 94, 1857–1861.
Trivedi, S., Zaman, S., Chaudhuri, T.R., Pramanick, P., Fazli, P., Amin, G., et al., 2016. Inter-annual Variation of salinity in Indian Sundarbans.
Twilley, R.R., Rivera-Monroy, V.H., 2009. Coastal Wetlands: An Integrated Ecosystem Approach. Ecogeomorphic models of nutrient biogeochemistry for mangrove wetlands, pp. 641–684.
Uddin, M.S., van Steveninck, EdR, Stuip, M., Shah, M.A.R., 2013. Economic valuation of provisioning and cultural services of a protected mangrove ecosystem: A case study on Sundarbans Reserve Forest, Bangladesh. Ecosyst. Serv. 5, 88–93.
Wahid, S.M., Babel, M.S., Bhuiyan, A.R., 2007. Hydrologic monitoring and analysis in the Sundarbans mangrove ecosystemBangladesh. J. Hydrol. 332, 381–395.
Ward, R.D., Friess, D.A., Day, R.H., MacKenzie, R.A., 2016. Impacts of climate change on mangrove ecosystems: a region by region overview. Ecosyst.Health Sustain. 2, e01211.
Win, S., Towprayoon, S., Chidthaisong, A., 2019. Adaptation of mangrove trees to different salinity areas in the Ayeyarwaddy Delta Coastal Zone, Myanmar. Estuar. Coast. Shelf Sci. 228, 106389.
Wright, I.J., et al., 2005. Modulation of leaf economic traits and trait relationships by climate. Glob. Ecol. Biogeogr. 14, 411–421. https://doi.org/10.1111/j.1466-822x.2005.00172.x.
Yoshikai, M., Nakamura, T., Suwa, R., Sharma, S., Rollon, R., Yasuoka, J., et al., 2021. Predicting mangrove forest dynamics across a soil salinity gradient using an individual-based vegetation model linked with plant hydraulics. Biogeosci. Discuss. 1–34.
Zhang, Y., Chen, H.Y.H., 2015. Individual size inequality links forest diversity and above-ground biomass. J. Ecol. 103, 1245–1252.
Zheng, L.T., Chen, H.Y.H., Yan, E.R., 2019. Tree species diversity promotes litterfall productivity through crown complementarity in subtropical forests. J. Ecol. 107, 1852–1861.